doi:10.1093/brain/aws302 Brain 2012: 135; 3645–3663 | 3645

BRAIN
A JOURNAL OF NEUROLOGY

Mapping preictal and ictal haemodynamic networks using video-electroencephalography and functional imaging

Umair J. Chaudhary,[1] David W. Carmichael,[2] Roman Rodionov,[1] Rachel C. Thornton,[1] Phillipa Bartlett,[1] Serge Vulliemoz,[3] Caroline Micallef,[4] Andrew W. McEvoy,[5] Beate Diehl,[1,6] Matthew C. Walker,[1] John S. Duncan[1] and Louis Lemieux[1]

1 Department of Clinical and Experimental Epilepsy, UCL Institute of Neurology, Queen Square, London WC1N 3BG, UK
2 Imaging and Biophysics Unit, UCL Institute of Child Health, London WC1N 1EH, UK
3 EEG and Epilepsy Unit, Clinical Neurology, University Hospitals of Geneva, rue Gabrielle-Perret-Gentil 4, CH-1211 Geneva14, Switzerland
4 Department of Neuroradiology and Neurophysics, National Hospital for Neurology and Neurosurgery Queen Square, London WC1N 3BG, UK
5 Department of Surgery, National Hospital for Neurology and Neurosurgery, Queen Square, London WC1N 3BG, UK
6 Clinical Neurophysiology, National Hospital for Neurology and Neurosurgery, Queen Square, London WC1N 3BG, UK

Correspondence to: Louis Lemieux,
MRI Unit, Epilepsy Society,
Chalfont St. Peter,
SL9 0RJ, UK
E-mail: louis.lemieux@ucl.ac.uk

Ictal patterns on scalp-electroencephalography are often visible only after propagation, therefore rendering localization of the seizure onset zone challenging. We hypothesized that mapping haemodynamic changes before and during seizures using simultaneous video-electroencephalography and functional imaging will improve the localization of the seizure onset zone. Fifty-five patients with $\geqslant$2 refractory focal seizures/day, and who had undergone long-term video-electroencephalography monitoring were included in the study. 'Preictal' (30 s immediately preceding the electrographic seizure onset) and ictal phases, 'ictal-onset'; 'ictalestablished' and 'late ictal', were defined based on the evolution of the electrographic pattern and clinical semiology. The functional imaging data were analysed using statistical parametric mapping to map ictal phase-related haemodynamic changes consistent across seizures. The resulting haemodynamic maps were overlaid on co-registered anatomical scans, and the spatial concordance with the presumed and invasively defined seizure onset zone was determined. Twenty patients had typical seizures during functional imaging. Seizures were identified on video-electroencephalography in 15 of 20, on electroencephalography alone in two and on video alone in three patients. All patients showed significant ictal-related haemodynamic changes. In the six cases that underwent invasive evaluation, the ictal-onset phase-related maps had a degree of concordance with the presumed seizure onset zone for all patients. The most statistically significant haemodynamic cluster within the presumed seizure onset zone was between 1.1 and 3.5 cm from the invasively defined seizure onset zone, which was resected in two of three patients undergoing surgery (Class I post-surgical outcome) and was not resected in one patient (Class III post-surgical outcome). In the remaining 14 cases, the ictal-onset phase-related maps had a degree of concordance with the presumed seizure onset zone in six of eight patients with structural-lesions and five of six non-lesional patients. The most statistically significant haemodynamic cluster was localizable at sub-lobar level within the presumed seizure onset zone in six patients. The degree of concordance of haemodynamic maps was significantly better ($P < 0.05$) for the ictal-onset phase [entirely concordant/concordant plus (13/20; 65%) + some concordance (4/20; 20%) = 17/20; 85%] than ictal-established [entirely concordant/concordant plus (5/13; 38%) + some concordance (4/13; 31%) = 9/13; 69%] and late ictal [concordant plus (1/9; 11%) + some concordance (4/9; 44%) = 5/9; 55%] phases. Ictal propagation-related haemodynamic changes were also seen in symptomatogenic areas (9/20; 45%) and the default mode network

Received June 6, 2012. Revised September 2, 2012. Accepted October 1, 2012

(13/20; 65%). A common pattern of preictal changes was seen in 15 patients, starting between 98 and 14 s before electrographic seizure onset, and the maps had a degree of concordance with the presumed seizure onset zone in 10 patients. In conclusion, preictal and ictal haemodynamic changes in refractory focal seizures can non-invasively localize seizure onset at sub-lobar/gyral level when ictal scalp-electroencephalography is not helpful.

Keywords: haemodynamic; electroencephalography; functional imaging; seizure; semiology; EEG-fMRI

Abbreviations: BOLD = blood oxygen level-dependent; ILAE = International League Against Epilepsy; FWE = family wise error; vEEG-fMRI = video-EEG and functional MRI

Introduction

Epilepsy surgery is potentially curative for refractory focal epilepsy, requiring rigorous presurgical evaluation to identify the seizure onset zone (Luders and Comair, 2000*a*) or network (Spencer, 2002). Synchronized video- and scalp-EEGs (video-EEG) are the standard approach to localize the seizure onset zone non-invasively (Rosenow and Luders, 2001) but has low sensitivity (25–56%) and spatial resolution compared with invasive EEG (Smith, 2005; Ray *et al*., 2007). Therefore, video-EEG may not localize the seizure onset zone (Lee *et al*., 2000; Remi *et al*., 2011; Catarino *et al*., 2012) warranting invasive recordings (Luders *et al*., 2006).

Recent advances in neuroimaging have significantly improved our ability to identify and localize structural abnormalities potentially involved in seizure generation. Nonetheless, these investigations are inconclusive in 25% of cases (Duncan, 2010), requiring other localization techniques. Functional MRI can map blood oxygen level-dependent (BOLD) changes over the whole brain with high spatial resolution in seizure-related areas (Jackson *et al*., 1994; Detre *et al*., 1995; Krings *et al*., 2000; Kubota *et al*., 2000). Simultaneously recorded scalp-EEG and functional MRI can reveal BOLD changes associated with interictal epileptiform discharges (Salek-Haddadi *et al*., 2006; Zijlmans *et al*., 2007; Thornton *et al*., 2011). Although recording seizures during EEG–functional MRI is limited by their unpredictable nature, difficulties with seizure identification inside the scanner and seizure-related motion effects (Chaudhary *et al*., 2011), ictal and preictal BOLD changes have been revealed in a few cases (Federico *et al*., 2005; Tyvaert *et al*., 2008; Donaire *et al*., 2009; Thornton *et al*., 2010). We have recently demonstrated synchronous video-EEG and functional MRI (Chaudhary *et al*., 2010) to identify and characterize seizures (Barba *et al*., 2007).

We investigated seizure-related haemodynamic changes for comparison with the seizure onset zone and post-surgical outcome where available in a series of patients with typical seizures during video-EEG–functional MRI. We hypothesized that (i) by partitioning seizures into phases, video-EEG–functional MRI can localize BOLD changes at the seizure onset better than in later parts of seizure, providing additional information at the sub-lobar level; (ii) brain networks recruited during later parts of seizure reflect seizure propagation; and (iii) focal or widespread brain networks, the latter reflected by multi-lobar haemodynamic patterns, can be recruited before the seizure onset (as determined from scalp-EEG) during the interictal to ictal transition.

Materials and methods

Subjects

Fifty-five patients with refractory focal seizures attending the National Hospital for Neurology and Neurosurgery, Queen Square, London, UK, were recruited prospectively from September 2008 to January 2012, and invited to undergo video-EEG–functional MRI scanning if they had (i) $\geqslant$2 seizures/day at the time of scanning; (ii) seizures previously recorded on long-term video-EEG monitoring; (iii) seizures that did not involve large seizure-related head motion; and (iv) no contraindications to undergo MRI scanning. All patients had a detailed clinical history taken, full neurological examination performed, MRI scanning (Duncan, 2010) and neuropsychology assessment. The clinical details and EEG findings for each patient with typical seizures during video-EEG–functional MRI are shown in Table 1 and Supplementary Table 1.

No drug reduction or sleep deprivation was used for video-EEG–functional MRI. A few patients had a known seizure trigger (Supplementary Appendix I). All subjects gave informed written consent, and the study was approved by the Joint Research Ethics Committee of the NHNN (UCLH NHS Foundation Trust) and UCL Institute of Neurology, Queen Square, London, UK. Functional MRI results for two patients (Patients 1 and 2) have previously been published in case reports (Centeno *et al*., 2011; Katschnig *et al*., 2011).

Six patients underwent intracranial electrode implantation as part of their presurgical evaluation based on hypotheses derived from spatial localization of ictal and interictal epileptiform discharges recorded during long-term video-EEG monitoring, structural abnormalities on MRI scans and other non-invasive investigations, such as PET, MEG or ictal SPECT where available. The invasive EEG was recorded using Nicolet EEG Neurodiagnostic System.

Data acquisition

Patients were asked to remain still during scanning, fitted with ear plugs, with their head immobilized using a vacuum cushion. Scalp-EEG (64-channel magnetic resonance-compatible cap: BrainCap-MR) was recorded synchronously with two video cameras during functional MRI scanning at the Epilepsy Society, Chalfont St. Peter, Buckinghamshire, UK. The video-EEG was displayed in real time (see Chaudhary *et al*., 2010, 2012 for set-up details).

Images were acquired using a 3 T GE Signa® Excite-HDX-Echospeed MRI scanner with a transmit/receive birdcage head coil. One to three 20-min echo-planar imaging (EPI) sessions were acquired (Table 2). The scanning was stopped prematurely in three cases (Patients 6, 9 and 18) to limit the risk of adverse incident. In four cases

Table 1 Clinical characteristics and localization of epilepsy

ID number	Gender	Age	Seizure onset (age)	Type of epilepsy	Seizure onset on scalp-EEG	MRI	seizure onset zone
Invasively defined seizure onset zone							
1	F	28	9	PLE	Regional right parieto-occipital	Multiple tubers: largest right parietal	Right parieto-occipital
3	M	19	2	Multifocal	Lateralized left hemisphere	focal cortical dysplasia: left parieto-occipito-temporal	Left parieto-occipito-temporal
10	F	32	2	Multifocal	Lateralized right max. Temporal	Ischaemic damage: right occipito-parietal	Right temporo-occipital
16	M	28	12	FLE	Regional left fronto-central	focal cortical dysplasia: left posterior SFG + MFG	Left frontal lobe
4	M	28	10	TLE	Regional left temporal	Non-lesional	Left temporal lobe
15	M	42	14	TLE	Lateralized left max. fronto-temporal	Non-lesional	Left temporal lobe
Presumed seizure onset zone							
5	F	23	10	Multifocal	Non-lateralized (fronto-central)	MCD: left frontal + parieto-temporal	Left frontal and parietal
8	F	31	6	Multifocal	Multi-regional	Right polymicrogyria and schizencephaly	Right hemisphere
11	F	20	11	FLE	Generalized max. right frontal	Ischaemic damage: right hemisphere	Right frontal lobe
12	F	24	9	Reflex	Regional fronto-central with left emphasis	focal cortical dysplasia: left paracentral lobule	Left frontal lobe
14	M	60	1	Hypothalamus	Non-localizable/lateralizable	Hypothalamic hamartoma	Hypothalamus
17	F	36	17	FLE	Regional right centro-parietal	focal cortical dysplasia: right MFG + precentral gyrus	Right frontal lobe
19	M	26	7	PLE	Regional right parieto-central	focal cortical dysplasia: right parietal-angular gyrus	Right parietal lobe
20	M	26	1	Hypothalamus	Non-localizable/lateralizable	Hypothalamic hamartoma	Hypothalamus
2	M	36	19	Reflex	Regional left centro-parietal	Non-lesional	Left centro-parietal
6	F	37	11	FLE	Non-lateralized (fronto-central)	Non-lesional	Medial frontal
7	F	44	1	FLE	Generalized, max. fronto-central	Non-lesional	Midline fronto-central
9	M	19	5	Reflex	Non-lateralized (fronto-central)	Non-lesional	Medial hemisphere
13	M	18	7	FLE	Generalized, max. right fronto-central	Non-lesional	Right frontal lobe
18	M	51	32	Reflex	Generalized, max. left fronto-temporal	Non-lesional	Left fronto-temporal

F = female; FLE = frontal lobe epilepsy; M = male; MCD = malformation of cortical development; MFG = middle frontal gyrus; PLE = parietal lobe epilepsy; TLE = temporal lobe epilepsy; SFG = superior frontal gyrus; focal cortical dysplasia = Focal cortical dysplasia.

Table 2 Seizures recorded during video-EEG–functional MRI

ID number	Seizure trigger	Video-EEG–functional MRI				
		Scan duration[a] (min)	Seizure identification	Seizures (*n*)	Ictal phases	Duration (s) Median (range)
1	None	80[b]	Video + EEG	1	Ictal onset	9
					Ictal established	15
2	Thinking or lifting weight in right hand	60	Video	24	Ictal	10 (2 s–3 min)
3	None	40	Video + EEG	2	Ictal onset	27 (24–30)
					Ictal established	11.5 (11–12)
					Late ictal	27.5 (27–28)
4	None	40	Video + EEG	7	Ictal onset	5.3 (2–9.2)
					Ictal established	4.9 (1.9–13.3)
					Late ictal	7.8 (7–9.4)
5	None	40	Video + EEG	4	Ictal onset	2.8 (2.8–10.4)
					Ictal established	6 (5.2–20)
					Late ictal	4.2 (4.2–16)
6	None	70[b]	Video + EEG	1	Ictal onset	9.8
					Ictal established	22.4
7	None	60	Video + EEG	30	Ictal onset	3.6 (1.4–8.6)
					Ictal established	14.1 (5.2–44.2)
					Late ictal	4.1 (1–13.2)
8	None	20	Video + EEG	6	Ictal	13.8 (8.9–20.4)
9	Rubbing right chest wall	75[b]	Video + EEG	2	Ictal onset	5.6 (2.9–8.4)
					Ictal established	9.7 (7.8–11.7)
					Late ictal	2
10	None	40	Video	1	Ictal	17
11	None	40	Video + EEG	17	Ictal onset	5 (2.4–8.8)
					Ictal established	7.8 (3–50.9)
					Late ictal	5.8 (3.1–18.5)
12	Movement of limbs	40	Video + EEG	15	Ictal	23.2 (13.7–34.6)
13	None	40	Video + EEG	4	Ictal	11.3 (8–17.3)
14	None	40	Video	1	Ictal	12
15	None	40	EEG	1	Ictal onset	5.7
					Ictal established	5
					Late ictal	17.4
16	None	80[b]	EEG	1	Ictal	39.5
					Ictal onset	9.7 (5–13.2)
					Ictal established	4.2 (2.6–8)
17	None	40	Video + EEG	10	Late ictal	8.1 (3.8–9.1)
18	Music	45	Video + EEG	1	Ictal onset	43.6
					Ictal established	10.4
19	None	40	Video + EEG	1	Ictal onset	6.2
					Ictal established	22.8
					Late ictal	11.2
20	None	40	Video + EEG	1	Ictal onset	7.6
					Ictal established	22.2

a Total duration of the video-EEG–functional MRI scanning session. One video-EEG–functional MRI session had 1–3 EPI sessions, each lasting 20 min.
b Patients had two vEEG-fMRI sessions on two different days to capture a seizure.

(Patients 1, 6, 9 and 16), the first video-EEG–functional MRI acquisition was unsuccessful at capturing seizures, and the acquisition was repeated on a different day; we also had flexible MRI scanning slots and scanned patients at times of the day when they reported that seizures were most likely to occur.

The EPI parameters were as follows: echo time = 30 ms, repetition time = 3000 ms, flip angle = 90°, slices = 44, slice thickness = 2.4 mm, gap = 0.6 mm, field of view = 24 × 24 cm^2 and matrix = 64 × 64. T_1-weighted MRI scans were also acquired at the same time (image parameters: echo time = 3.1 ms, repetition time = 8.3 ms, inversion time = 450 ms, flip angle = 20°, slices = 170, slice thickness = 1.1 mm, field of view = 24 × 18 and matrix = 256 × 256 cm^2).

Data processing and analysis

Electroencephalography and functional magnetic resonance imaging processing

EEG was corrected offline for scanner and pulse-related artefacts (Allen *et al.*, 1998, 2000) using BrainVision Analyzer2 (BrainProducts).

Video-EEG recorded during video-EEG–functional MRI was reviewed jointly by U.C. and experienced neurophysiologists (B.D., S.V. and M.W.) to identify interictal epileptiform discharges and ictal rhythms (Luders *et al*., 2000*b*; Foldvary *et al*., 2001) and semiology (Luders *et al*., 1998) and to compare with long-term video-EEG monitoring. The seizures were partitioned into phases based on spatio-temporal evolution (Niedermeyer and Lopes da Silva, 2005) of ictal EEG changes and semiology on video to attempt to distinguish onset from propagation-related BOLD changes. The ictal phases (Thornton *et al*., 2010) and preictal time window were defined as follows:

Preictal: 30 s preceding the ictal onset phase (see below) on scalp-EEG without any EEG changes. In cases without clear electrographic signature or EEG obscured by myogenic artefact, the preictal phase was defined as 30 s before the first semiological change was observed on video.

Ictal onset: build-up of ictal EEG pattern (Foldvary *et al*., 2001) on scalp EEG preceding clinical features.

Ictal established: onset of the clinical manifestations along with regional/generalized EEG changes or emergence of myogenic artefact on scalp-EEG.

Late ictal: subsequent EEG slowing following the ictal-established phase.

Seizures that did not have an electrographic signature (e.g. simple partial seizures; Binnie *et al*., 1999; Smith, 2005), or for which the ictal phases could not be separated clearly because of myogenic artefact on EEG, were labelled as a single ictal phase.

Physiological activities, including spontaneous eye blinks/movements, swallowing, jaw clenching, head jerk, facial twitches and brief hand/foot movements, were identified on video EEG and distinguished from ictal semiology by comparison with ictal events captured on long-term video-EEG monitoring (Chaudhary *et al*., 2012).

The functional MRI data were analysed using Statistical Parametric Mapping (SPM5, http://www.fil.ion.ucl.ac.uk/spm). After discarding the first of our image volumes (T_1-saturation effect), the EPI images were realigned and spatially smoothed using an isotropic Gaussian kernel of 8-mm full-width at half-maximum (Friston *et al*., 1995*a*).

Functional magnetic resonance imaging modelling

The functional MRI data during which seizures were recorded were analysed within the general linear model framework to map preictal and ictal haemodynamic changes. Eleven patients had more than one seizure during video-EEG–functional MRI, out of which seven had seizures in more than one EPI session, which were included in a single general linear model as separate sessions. Two models were used to investigate the BOLD changes associated with the ictal and preictal phases.

In Model 1 (ictal changes), each ictal phase was represented mathematically as variable duration block in a separate regressor. We sought to identify putative BOLD patterns consistent across seizures. Therefore, in a case with multiple seizures of similar electro-clinical characteristics, we modelled a particular ictal phase from multiple seizures within single regressor. To explain as much of BOLD signal variance as possible, this model also included regressors (Chaudhary *et al*., 2012) representing: interictal epileptiform discharges (herein treated as confounds), physiological activities (each type of earlier-described activity modelled as variable duration block), motion (inter-scan realignment parameters and their Volterra expansion; Friston *et al*., 1996) and cardiac pulse (Liston *et al*., 2006). Each interictal epileptiform discharge type was modelled as a separate confound; individual interictal epileptiform discharges were represented as stick functions and runs as blocks. Data sets were analysed irrespective of the amount of head motion. Ictal phases, interictal epileptiform discharges and physiological activities were convolved with the canonical haemodynamic response function and its temporal and dispersion derivatives. The functional MRI data were high-pass filtered (cut-off: 128 s).

In Model 2 (preictal changes: spontaneous seizures only), a more flexible approach based on the Fourier basis set was used to model BOLD changes during the preictal time window defined as 30 s before the ictal onset phase. The basis set order was set to five (combination of five sine and five cosine functions), which is equal to the preictal time window length/2 $\times$ repetition time = 6 s. Thus, Fourier basis set captured arbitrarily shaped fluctuations over time scales down to 2 $\times$ repetition time, and was not set to zero at the window start and end to capture the actual onset of BOLD changes if they extend beyond the modelled window. The remainder of Model 2 consisted of Model 1, and was treated as the nuisance effects.

Assessment of blood oxygen level-dependent change significance, visualization and level of concordance

SPM[F]-maps were obtained for each ictal phase separately and across combined all ictal phases for Model 1 and for the preictal phase for Model 2 at conventional conservative threshold: $P < 0.05$, corrected for family wise-error. When BOLD changes were not seen at $P < 0.05$, we used a less conservative statistical threshold: $P < 0.001$, uncorrected. The resulting maps were co-registered with the patient's anatomical MRI scan. The fitted BOLD time course for each cluster was plotted and classified as increases, decreases or biphasic (including both increases and decreases) according to the sign of the peak change relative to baseline.

To test Hypothesis 1, the presumed seizure onset zone was defined non-invasively at the lobar level on the basis of interictal epileptiform discharges, ictal rhythm, ictal semiology and structural abnormality where available. The ictal BOLD maps were compared with the presumed seizure onset zone with an experienced neuroradiologist (C.M.) and classified on the basis of the most statistically significant cluster (global-maximum) and other clusters as: entirely concordant (all BOLD clusters in the same lobe as and within 2 cm of the presumed seizure onset zone), concordant plus (the global-maximum cluster was in the same lobe as and within 2 cm of the presumed seizure onset zone, and other clusters were remote from the presumed seizure onset zone), some concordance (the global-maximum cluster was remote from the presumed seizure onset zone, and one of the other clusters was in the same lobe as and within 2 cm of the presumed seizure onset zone) and discordant [all clusters were remote (different lobe or opposite hemisphere) from the presumed seizure onset zone].

The BOLD clusters located in the ventricular system, vascular tree, edges and base of brain and cerebellum were not considered (Chaudhary *et al*., 2012). First, for patients who underwent invasive EEG recording during presurgical assessment, we confirmed the sub-lobar localization provided by video-EEG–functional MRI with the invasively defined seizure onset zone. We measured the Euclidean distance between the statistical maximum voxel of global-maximum/other BOLD cluster, within the presumed seizure onset zone for the ictal onset/ictal phase and the invasively defined seizure onset zone. The invasively defined seizure onset zone was delineated by two experienced neurophysiologists (B.D. and M.W.) as the location of depth/grid contacts on invasive EEG where the first and maximal ictal changes were seen. Second, for patients who did not undergo invasive EEG, we compared the sub-lobar localization of global-maximum BOLD cluster provided by video-EEG–functional MRI with the level of localization provided by ictal rhythm on scalp-EEG. Third, we compared the level of concordance of BOLD maps with the presumed seizure onset zone between different ictal phases using Spearman's rank correlation (r_s) (IBM SPSS Statistics).

To test Hypothesis 2, we assessed first the ictal established/ictal phase-related BOLD maps in relation to the symptomatogenic areas (defined on the basis of specific ictal semiology for each patient, see Supplementary Table 1). We also compared the presence/absence of changes in symptomatogenic and non-symptomatogenic areas using Fisher's exact test (IBM SPSS Statistics). Second, we combined all ictal BOLD maps in relation to the resting state networks (Damoiseaux *et al*., 2006; Mantini *et al*., 2007; van den Heuvel *et al*., 2009). We also tested for the relationship between presence/absence of loss of consciousness (as reported during long-term video-EEG monitoring for typical seizures) and BOLD changes in the default mode network using mean contingency coefficient (Φ), and in the subgroup with BOLD decreases in the default mode network, we tested for the association of BOLD decreases with loss of consciousness using non-parametric chi-squared test (IBM SPSS Statistics).

To test Hypothesis 3, the preictal haemodynamic onset was defined as the time at which the fitted response was more than two standard deviations above or below baseline. The concordance of preictal maps was evaluated as per aforementioned concordance scheme. A secondary assessment of the preictal changes was performed having found that the fitted values at the start of the modelling window were generally not zero. We inspected the fitted time courses, for each preictal BOLD cluster (>5 voxels) and each seizure, for the period preceding the modelled preictal time window (i.e. backwards from −30 s from the ictal onset phase) visually to determine the time at which the preictal changes were significantly different from zero and later continued into the modelled preictal time window. We also compared the level of concordance of ictal onset/ictal phase-related and preictal BOLD maps with the presumed seizure onset zone using Spearman's rank correlation (r_s) (IBM SPSS Statistics).

Results

Twenty-four of the 55 patients reported having ictal events during video-EEG–functional MRI, and 20 of 55 patients (36.3%) had typical seizures during video-EEG–functional MRI. None of the patients with typical seizures during video-EEG–functional MRI reported an atypical event; four patients with atypical events are not considered further. Of the 20 cases with typical seizures, six had frontal lobe, four had focal reflex, four had multifocal, two had temporal lobe, two had parietal lobe and two had hypothalamic seizures; their median age was 28 years (range 18–60 years), median seizure onset was at 9 years (range 1–32 years) and there were 12 males.

The video-EEG–functional MRI scanning time (median = 40 min; range 20–80 min) and seizure statistics for each patient are described in Table 2. The seizures were identified on video-EEG in 15 of 20 patients (75%), on EEG only in 2 of 20 patients (10%, technical video failure) and on video only in 3 of 20 patients (15%, no ictal EEG change or EEG obscured by myogenic artefact). In 13 of 20 patients (65%), distinct ictal phases could be identified and the remainder had single ictal phase.

Ictal blood oxygen level-dependent changes

Statistically significant BOLD changes were revealed for all ictal phases except for Patient 3 for late ictal phase. BOLD changes were seen at $P < 0.05$ (corrected for family-wise error) in 15 of 20 patients (75%) for all ictal phases, and at $P < 0.001$ (uncorrected) for one of the ictal phases in the remaining five patients.

Overall, the level of concordance of the BOLD maps with the presumed seizure onset zone (Fig. 1A) was better for the ictal onset/ictal phase [entirely concordant/concordant plus (13/20; 65%) + some concordance (4/20; 20%) = 17/20; 85%] than ictal established [entirely concordant/concordant-plus (5/13; 38%) + some concordance (4/13; 31%) = 9/13; 69%] and late ictal phases [concordant plus (1/9; 11%) + some concordance (4/9; 44%) = 5/9; 55%)], and was significantly correlated with the ictal onset/ictal phase ($r_s = 0.3$, $P < 0.05$).

Comparison of ictal blood oxygen level-dependent changes with the invasively defined seizure onset zone and surgical outcome

In the six patients (Patients 1, 3, 4, 10, 15 and 16) who underwent invasive EEG recordings, four had epileptogenic structural abnormalities: focal cortical dysplasia (Patients 3 and 16), tuberous sclerosis (Patient 1) and ischaemic damage (Patient 10) (Table 1). For these four patients, BOLD changes were seen within the presumed seizure onset zone (Table 3) overlapping the structural abnormalities (Fig. 1B and C). Ictal onset/ictal phase-related maps were classified as entirely concordant/concordant plus in three and to have some concordance in one patient. Two of these four patients had ictal established phases, and the maps were classified as entirely concordant/concordant plus and to have some concordance for one patient each.

For two patients (Patients 4 and 15) who underwent invasive EEG recordings and did not have structural abnormalities also showed BOLD changes within the presumed seizure onset zone (Table 3) at sub-lobar level. The ictal onset/ictal phase-related maps were classified as entirely concordant/concordant plus (Fig. 2A) in two patients; ictal established phase-related maps were classified to have some concordance in one patient and were discordant in one patient and late ictal phase-related maps were classified as concordant plus and to have some concordance for one patient each.

The distance between the ictal onset/ictal phase-related global-maximum cluster within the presumed seizure onset zone, and the invasively defined seizure onset zone was 1.1–3.5 cm in five of six patients (Table 3; Fig. 1B and C), demonstrating that video-EEG-functional MRI can localize the seizure onset zone at sub-lobar level non-invasively. Three patients proceeded to surgery, and the BOLD cluster within the presumed seizure onset zone was resected in two patients [Patients 1 and 16: International League Against Epilepsy (ILAE) Class I post-surgical outcome; Fig. 1B and C], and was not resected in one patient (Patient 4: ILAE Class III post-surgical outcome; Fig. 1B and C).

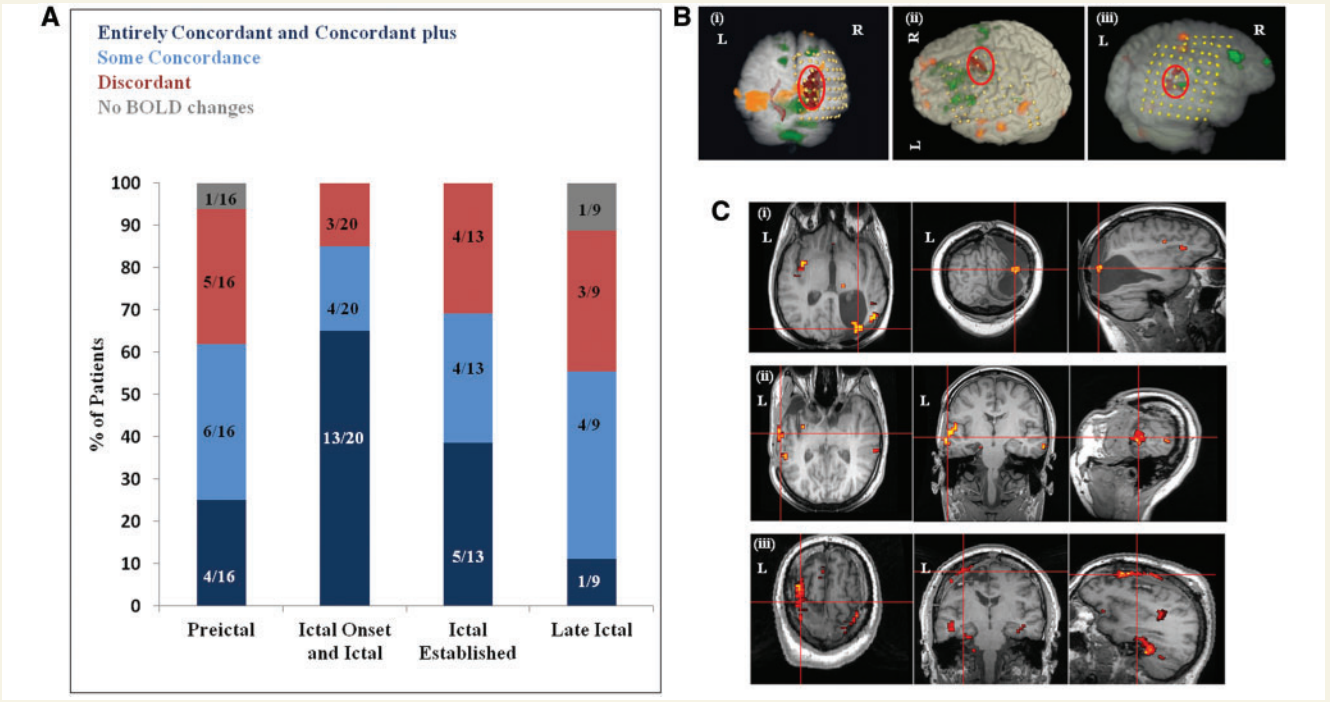

Figure 1 Ictal and preictal BOLD changes and their comparison with the seizure onset zone and cortical resection. (**A**) Bar chart showing level of concordance of BOLD changes with the presumed seizure onset zone, during ictal and preictal phases. (**B**) SPMs of F-statistics overlaid on 3D rendered brain in individual space, showing the relationship between preictal (orange) and ictal onset phase-related BOLD changes (green), implanted electrodes and structural lesion (red). (**Bi**) Patient 10: the global-maximum cluster in the right occipito-temporal region for the preictal and ictal phase was within the presumed seizure onset zone and was 2.5 and 1.8 cm, respectively, from the invasively defined seizure onset zone. (**Bii**) Patient 16: the global-maximum cluster in the left superior/middle frontal gyrus for the ictal phase was within the presumed seizure onset zone at 1.5 cm from the invasively defined seizure onset zone. For the preictal phase another cluster in medial superior frontal gyrus was within the presumed seizure onset zone at 2.5 cm from the invasively defined seizure onset zone. (**Biii**) Patient 1: for the ictal onset phase, the second most statistically significant BOLD cluster in right inferior parietal lobe was within the presumed seizure onset zone at 1.9 cm from the invasively defined seizure onset zone. The global-maximum preictal cluster in the right parietal region was within the presumed seizure onset zone at 3 cm from the invasively defined seizure onset zone. (**C**) ictal onset phase-related maps overlaid on co-registered post-surgical T_1-volume. Cross-hair shows the BOLD cluster within the presumed seizure onset zone. (**Ci**) Patient 1 had a cortical resection including the right parietal tuber and overlapping ictal onset phase-related cluster (cross-hair; ILAE Class I at 1.5 year). (**Cii**) Patient 4 underwent left anterior temporal lobe resection, which did not involve the ictal onset phase-related global-maximum cluster in superior temporal gyrus (cross-hair; ILAE Class III at 1 year). (**Ciii**) Patient 16 had a resection including right posterior superior frontal gyrus/MFG and part of supplementary motor area and ictal onset phase-related global-maximum cluster (cross-hair; ILAE Class I at 1 year).

Comparison of ictal blood oxygen level-dependent changes with the presumed seizure onset zone

In the 14 patients who did not undergo invasive EEG recordings, eight had epileptogenic structural abnormalities: focal cortical dysplasia (Patients 12, 17 and 19), hypothalamic hamartoma (Patients 14 and 20) and other abnormalities (Patients 5, 8 and 11) (Table 1). For these eight patients, BOLD changes were seen within the presumed seizure onset zone overlapping the structural abnormalities. The ictal onset/ictal phase-related maps were classified as (Table 3; Fig. 2B): concordant plus = 5/8, some concordance = 1/8 and discordant = 2/8. The ictale stablished phase was seen in 5 of 8 patients with structural abnormalities, and the maps were classified as: concordant plus = 2/5, some concordance = 2/5 and discordant = 1/8. The late ictal phase was seen in 4 of 8 patients with structural abnormalities, and the maps were classified as: some concordance = 2/4 and discordant = 2/4.

Six patients (Patients 2, 6, 7, 9, 13 and 18) who did not undergo invasive EEG recordings and also did not have structural abnormalities showed BOLD changes within the presumed seizure onset zone (defined on the basis of interictal and ictal discharges on EEG and ictal semiology) at sub-lobar level. The ictal onset/ictal phase-related maps were classified as entirely concordant/concordant plus in three, some concordance in two and discordant in one patient. The ictal established phase was seen in 4 of 6 patients, and the maps were classified as: concordant plus = 2/4 and discordant = 2/4. The late ictal phase was seen in 2 of 6 patients, and the maps were classified as: some concordance = 1/2 and discordant = 1/2.

For the 8 of 14 patients with entirely concordant/concordant plus BOLD maps for the ictal onset/ictal phase, the global-maximum BOLD cluster was localizable, within the presumed

Table 3 Localization of ictal BOLD changes and level of concordance with the seizure onset zone

ID number	Localization of BOLD changes for each ictal phase (increases = ↑, decreases = ↓)								Level of concordance with the presumed seizure onset zone	Invasively defined seizure onset zone	¬ Idl (cm)
	Phase	R frontal	R temporal	R parietal	L frontal	L temporal	L parietal	Others			
Invasively defined seizure onset zone											
1	IO	↑**MFG**		↑Inferior[a]					Some concordance	R parieto-occipital tuber	7/1.9
	IE	↑**MFG**		↑Inferior					Some concordance		
3	IO				↓**MFG/IFG**[a]		↓Superior[a]		Concordant plus	seizure onset zone 1: L TPO	seizure onset zone 1: 4.6/1.7
	IE			↑Superior	↑MFG		↑**Superior**	-	Concordant plus	seizure onset zone 2: L Posterior temporal seizure onset zone 3: L IFG	seizure onset zone 2: 4 seizure onset zone 3: 2.3
10	Ictal			↑Superior			↑Superior	↑**R TPO**[a] ↑Med.Occ. ↑Precuneus	Concordant plus	seizure onset zone 1: R hippocampus seizure onset zone 2: Medial TPO	seizure onset zone 1: 5.6 seizure onset zone 2: 1.8
16	Ictal			↑Superior	↓**SFG/MFG**[a,b]	↓STG	↑Superior, ↓SMG	↓Precuneus	Concordant plus	Left superior frontal sulcus and Posterior SFG	1.5
4	IO					↑**STG**[a]			Entirely concordant	L anterior ITG	3.5
	IE	↑**MFG**			↑MFG				Discordant		
	Late ictal					↓**Posterior**			Concordant plus		
15	IO				↑MFG, MC	↑**STG**[a]			Concordant plus	seizure onset zone 1: L temporal pole	seizure onset zone 1: 1.1
	IE				↓MFG	↑**STG**[b]			Some concordance	seizure onset zone 2: L ITG	seizure onset zone 2: 3
	Late ictal				↑***MFG***	↑*Post. temporal STG*			Some concordance		
Presumed seizure onset zone											
5	IO						↑***Inferior***[a]	↑*Precuneus*	Concordant plus	NA	NA
	IE				↓ **L fronto-temporo-parietal**				Concordant plus	NA	NA
	Late ictal	↑FP, ↑Med.SFG			↑**FC,** ↑FP, ↑Med.SFG				Discordant	NA	NA
8	Ictal	↑MFG[b], ↓Med.SFG	↑**MTG**[a]						Concordant plus	NA	NA
11	IO	↑**R MFG**[a]		↑Superior	↑L MFG		↑Superior		Concordant plus	NA	NA
	IE							↓**Precuneus**	Discordant	NA	NA
	Late ictal	↑*IFG*	↑***Lateral parieto-temporal***						Some concordance	NA	NA
12	Ictal	↓MFG			↓**MFG/SFG**[a]	↓Temporo-occipital			Concordant plus	NA	NA
14	Ictal	↓MFG			↓MFG	↓**STG**		↓Paracentral lobule	Discordant	NA	NA

(continued)

Table 3 Continued

ID number	Localization of BOLD changes for each ictal phase (increases = ↑, decreases = ↓)								Level of concordance with the presumed seizure onset zone	Invasively defined seizure onset zone	¬ ldl (cm)
	Phase	R frontal	R temporal	R parietal	L frontal	L temporal	L parietal	Others			
17	IO	↑**MC**[a]**, SMA, SFG**		↓Superior			↓Superior	↓Paracental lobule, precuneus	Concordant plus	NA	NA
	IE	↑MC[b], Med.SFG		↑Superior	↑MC[b], Med.SFG		↑Superior	↑**Paracentral lobule** Precuneus	Some concordance	NA NA	NA NA
	Late ictal	↓**MTG**					↓Superior		Discordant	NA	NA
19	IO	↑**MFG** ↓Med.SFG		↓SMG[a]	↓Med.SFG				Some concordance	NA NA	NA NA
	IE	↓MFG ↓Med.SFG		↓**SMG** ↓Superior	↓MFG, ↓Med.SFG		↓Superior	↓Precuneus	Concordant plus	NA NA	NA NA
	Late ictal	↓MFG ↓Med.SFG		↓SMG ↓**Superior**	↓MFG ↓Med.SFG			↓Precuneus	Some concordance	NA	NA
20	IO		↑Med.Temp.		↑MC	↑Med.Temp.	↑**Superior**		Discordant	NA	NA
	IE	↓Med.SFG			↓MFG, MC		↓**Med.Temp.**	↓Hypothalamus	Some concordance	NA	NA
2	Ictal				↑***MC (hand area)***[a,b]				Entirely concordant	NA	NA
6	IO				↓**SFG, MC**[a]				Entirely concordant	NA	NA
	IE				↓***SFG, MC***[b]				Entirely concordant	NA	NA
7	IO	↓**Med.SFG**[a]		↓Superior	↓**Med.SFG**[a]				Concordant plus	NA	NA
	IE	↓Lateral frontal, ↓Med.SFG[a]		↓**Superior**	↓Lateral frontal ↓Med.SFG[a]		↓Superior	↓Precuneus, ↓cingulum[b], ↑thalamus	Discordant	NA	NA
	Late ictal	↓Lateral frontal, ↓Med.SFG[a]		↓**Superior**	↓Lateral frontal, ↓Med.SFG[a]		↓Superior	↓Precuneus	Discordant	NA	NA
9	IO		↓**MTG**		↓Med.SFG[a]				Some concordance	NA	NA
	IE	↑MFG/IFG[b]	↑MTG		↑**Med.SFG**[b]	↑MTG			Concordant plus	NA	NA
	Late ictal		↓**MTG**		↓Med.SFG				Some concordance	NA	NA
13	Ictal			↑**Superior**					Discordant	NA	NA
18	IO	↓**MFG** Med.SFG		↓Superior	↓Med.SFG	↓STG[a]			Some concordance	NA	NA
	IE	↓**MFG**		↓Superior				↓Precuneus	Discordant	NA	NA

BOLD changes for different ictal phases are described at $P < 0.05$ (FWE-corrected) in 15 patients. In five patients, one of the ictal phase revealed BOLD changes at less conservative statistical threshold $P < 0.001$ uncorrected for FWE only (italicized). For each ictal phase the most statistically significant cluster (global-maximum) is in bold.

a IO/ictal phase-related BOLD cluster highlighted non-invasively to be within the presumed seizure onset zone.

b IE/ictal phase-related BOLD cluster within the symptomatogenic area as defined on the basis of ictal semiology.

¬ldl = distance (cm) between the intracranial electrode with first EEG change at seizure onset and global-maximum/nearest BOLD cluster for the 'Ictal onset'/'ictal' phase highlighted non-invasively to be within the presumed seizure onset zone.

IE = Ictal established; IFG = inferior frontal gyrus; IO = ictal onset; ITG = inferior temporal gyrus; L = left; MC = motor cortex; Med.SFG = medial SFG; MTG = middle temporal gyrus; Occ. = Occipital; R = right; SMA = supplementary motor area; STG = superior temporal gyrus; Temp. = temporal; TPO = temporo-parieto-occipital junction; NA = not applicable.

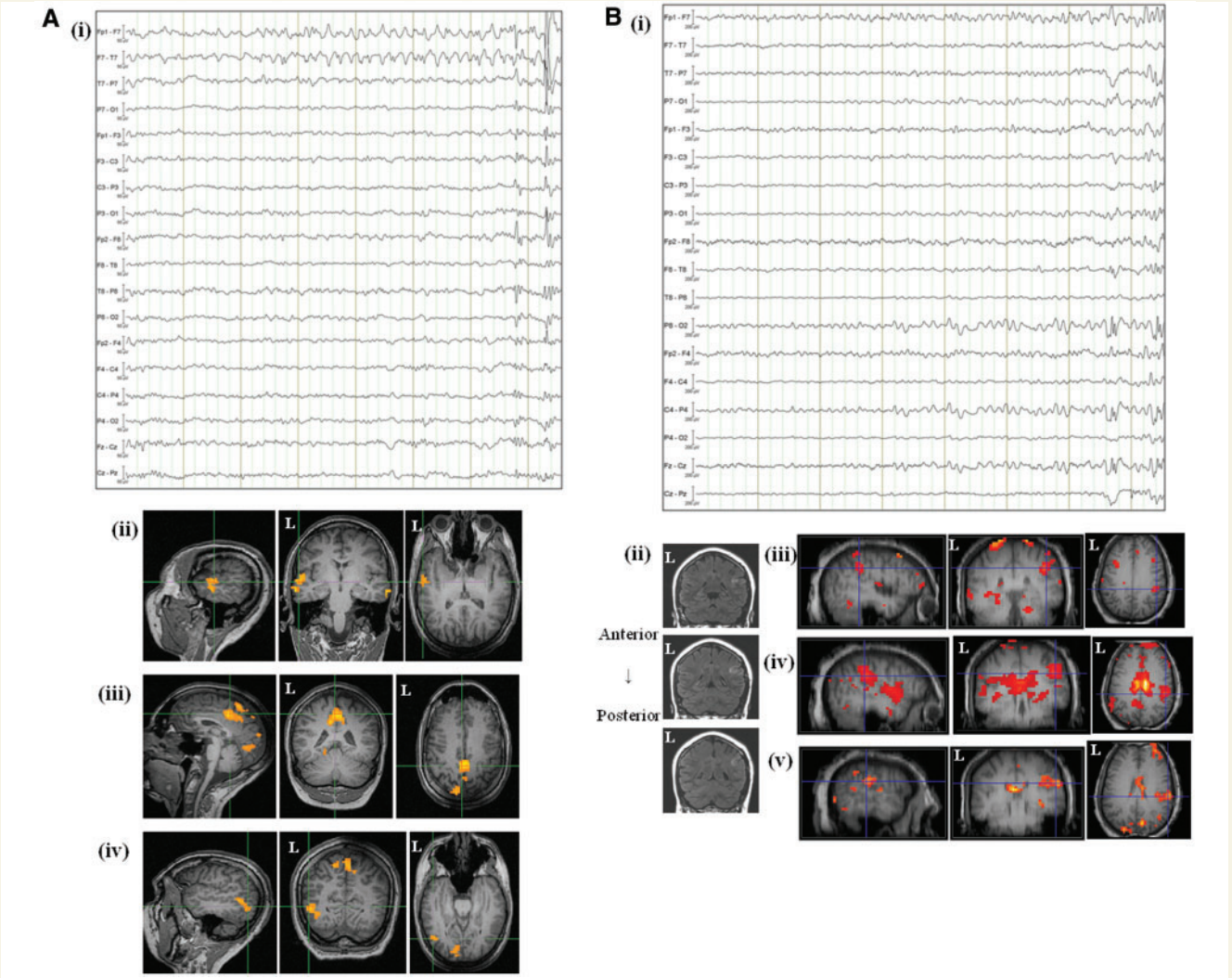

Figure 2 Comparison of ictal phase-related BOLD changes with presumed seizure onset zone. (**A**) Patient 4. (**Ai**) Representative EEG sample recorded inside scanner showing a regional left temporal ictal pattern at seizure-onset (F7, T7). (**Aii–iv**) BOLD changes overlaid on to T_1-volume. (**Aii**) Ictal onset phase-related concordant plus map showing the global-maximum cluster: left superior temporal gyrus (cross-hair) within the presumed seizure onset zone. (**Aiii**) Ictal established phase-related discordant map showing changes in right superior andMFG, basal ganglia, left cuneus and paracentral lobule (cross-hair). (**Aiv**) Late ictal phase-related concordant plus map showing global-maximum cluster: left posterior temporal region within the presumedseizure onset zone. (**B**) Patient 19. (**Bi**) Representative EEG sample recorded inside scanner showing a regional right centro-parietal ictal pattern. (**Bii**) focal cortical dysplasia in the right supra-marginal gyrus (SMG) on MRI scan. (**Biii–v**) BOLD changes overlaid on to T_1-volume. (**Biii**) Ictal onset phase-related map with some concordance showing global-maximum cluster in rightMFG, and another cluster in right SMG (cross-hair) within the presumed seizure onset zone. (**Biv**) Ictal established phase-related concordant plus map showing global-maximum cluster in right SMG (cross-hair) within the presumed seizure onset zone. BOLD changes within the ventricles were discounted for concordance classification. (**Bv**) Late ictal phase-related map with some concordance showing global-maximum cluster in right parietal lobe and another cluster in SMG (cross-hair) within the presumed seizure onset zone.

seizure onset zone, to one or two gyri in six patients (Patients 2, 6, 7, 8, 11 and 12), and spanned more than two gyri within the same lobe in the remaining two patients (Patients 5 and 17). In comparison, using the criteria set out in Luders *et al*. (2000*b*), the seizure onset scalp-EEG pattern was localized to one lobe (Patients 2, 12 and 17) or multiple lobes (Patients 5, 6, 7, 8 and 11; Table 1). Moreover, in six patients with frontal lobe seizures and difficult to localize ictal EEG, the global-maximum ictal onset phase-related BOLD cluster was localized within the presumed seizure onset zone at sub-lobar level in four patients.

Ictal propagation-related blood oxygen level-dependent networks

BOLD changes were revealed in symptomatogenic areas and/or eloquent cortex in 9 of 20 patients (45%; Table 3) for ictal established/ictal phases. Three patients had BOLD changes only in symptomatogenic areas, and the rest also had changes in non-symptomatogenic areas. The two groups with changes in symptomatogenic and non-symptomatogenic areas were not statistically significantly different. These areas included motor cortex for hand,

foot or face movements (Patients 2, 6 and 17), supplementary motor area/prefrontal cortex for 'figure of 4' sign (Patient 9), medial or lateral temporal lobes in temporal lobe epilepsy for automatisms (Patient 15), precentral gyrus and posterior middle frontal gyrus for eye deviation and head turning (Patients 8, 9 and 16) hypothalamus for gelastic seizures (Patient 20) and thalamus, limbic temporal structures, cingulum and medial frontal for dialeptic seizures (Patient 7).

In relation to the resting state networks (Mantini *et al*., 2007), BOLD changes were seen in the precuneus/cuneus, bilateral parietal lobes, posterior cingulate and/or medial frontal lobes reflecting the default mode network (Raichle *et al*., 2001) in 13 of 20 patients (65%; Fig. 3A and Supplementary Table 2) for combined all ictal phases. These were BOLD decreases in 11 patients and increases in two patients. We did not measure the impairment of consciousness during video-EEG–functional MRI; however, we compared the association of BOLD changes in the default mode network with the loss of consciousness assessed during long-term video-EEG monitoring for typical seizures (Fig. 3B). We found a moderate correlation ($\Phi = 0.3$) between the presence of BOLD changes in the default mode network and the loss of consciousness that was not statistically significant. However, in the subgroup of patients with BOLD decreases in the default mode network, these changes were significantly associated with the loss of consciousness ($P < 0.05$). We also found BOLD changes in relation to other resting state networks (Supplementary Appendix II) at $P < 0.001$, uncorrected for family-wise error.

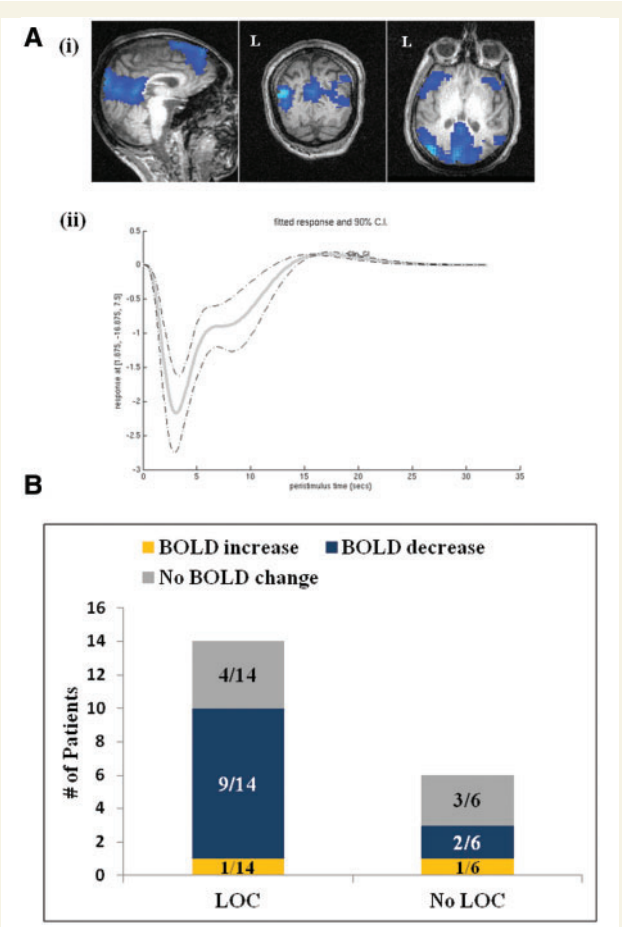

Figure 3 BOLD changes in the default mode network. (**A**) Patient 7. (**Ai**) SPM[F] map for combined all ictal (across whole seizure) overlaid on co-registered T_1-volume showing BOLD decreases in precuneus, cuneus, bilateral superior parietal, bilateral dorsolateral frontal and medial frontal cortex reflecting default mode network. (**Aii**) Predicted BOLD response based on the maximum likelihood parameter estimates of the general linear model for the maximum BOLD change in precuneus showing BOLD decrease. (**B**) Bar chart showing the proportion of patients with BOLD increases and decreases and loss of consciousness during seizures.

Preictal blood oxygen level-dependent changes

Preictal changes were investigated in 16 of 20 patients (80%) who had spontaneous seizures (Table 4). Statistically significant preictal changes were revealed at $P < 0.05$ (corrected for family-wise error) in 2 of 16 patients only and at $P < 0.001$ (uncorrected) for 15 of 16 patients (93.7%). One patient (Patient 17) did not show any preictal changes.

Preictal maps were classified as: concordant plus = 4/16 (25%), some concordance = 6/16 (37.5%) and discordant = 5/16 (31.2%) (Table 4; Fig. 4). The level of concordance of the BOLD maps (Fig. 1A) for the ictal onset/ictal phase (85%) was better than preictal phase (10/16; 62.5%), and was significantly correlated with the ictal onset/ictal phase ($r_s = 0.4$, $P < 0.05$).

Inspection of the preictal time courses across 74 seizures in 15 patients revealed that the onset of BOLD changes varied from 98 to 14 s before the electrical seizure onset during video-EEG–functional MRI (Fig. 4; Table 4). There was a consistent pattern of BOLD decrease (range −98 to −14 s) followed by a BOLD increase (range −50 to 0 s). The median onset for preictal BOLD decreases was −31 s [95% confidence interval (CI) −35.7 to −26.3 s], and the median onset for preictal BOLD increase was −16 s (95% CI −18.1 to −13.9 s).

Direction of blood oxygen level-dependent change

The BOLD maps for the individual ictal phases contained clusters corresponding to a mixture of BOLD increases and decreases in 11 of 20 patients, increases only for four patients and decreases only for five patients (Table 3). For the patients with entirely concordant/concordant plus BOLD maps, the global-maximum cluster corresponded to BOLD increase in 8 of 13 patients for the ictal onset/ictal phase, 2 of 5 patients for the ictal established phase and none for the late ictal phase. The BOLD clusters for ictal established and late ictal phases were remote from the seizure onset zone and were predominantly decreases (Table 3).

Discussion

We demonstrated the application of video-EEG–functional MRI in patients with frequent refractory focal seizures and identified

Table 4 Localization of preictal BOLD changes and level of concordance with the seizure onset zone

ID number	Preictal BOLD changes Positive = ↑, negative = ↓, biphasic = ↑↓	Level of concordance with the presumed seizure onset zone	Onset of preictal BOLD changes (sec)		Delay between electrographic and clinical seizure onset on intracranial EEG (s)
			↓	↑	
1	↓↑*R superior parietal, L parieto-temporal, medial frontal, L temporal*	Concordant plus	−79	−32	3
3	↓↑*L occipito-temporal, L temporal-ITG, L motor-cortex, R ITG, B/L medial occipital*	Concordant plus	−30 to −28	−18 to −17	25
4	↓↑*R orbito-frontal, R temporal-STG, post. cingulate, R cuneus, L temporal-MTG*	Some concordance	−80 to −20	−26 to 0	8
5	↓↑B/L fronto-central-SFG/MFG/Med.SFG	Discordant	−90 to −14	−50 to −1	NA
6	↓↑*R frontal lobe-MFG/IFG, R precuneus, R superior parietal*	Discordant	−37	−20	NA
7	↓↑ *L temporal, L frontal-motor-cortex*	Some concordance	−84 to −19	−25 to −3	NA
8	↓↑*R frontal-SFG, R temporal-STG*	Concordant plus	−74 to −52	−25 to −23	NA
10	↓↑*L medial parieto-occipital, R medial parieto-occipital, B/L parieto-occipital*	Some concordance	−53	−28	38
11	↓↑*R cingulate, R frontal-SFG, R orbito-frontal*	Concordant plus	−40 to −17	−18 to −5	NA
13	↓↑*R temporal, L temporo-occipital*	Discordant	−68 to −28	−30 to −28	NA
14	↓↑L temporal-MTG	Discordant	−98	−25	NA
15	↓↑*L fronto-polar, L frontal-MFG, L temporal-STG*	Some concordance	−25	−4	13
16	↓↑*R temporal-MTG, L temporal-MTG, medial frontal-SFG, L posterior temporo-occipital, L parietal, medial occipital, L frontal-SFG*	Some concordance	−67	−25	6
19	↓↑*R frontal-IFG/MFG/SFG, B/L temporal-MTG, R frontal-motor-cortex, paracentral lobule, R parietal-SMG, Medial frontal*	Some concordance	−37	−30	NA
20	↓↑ *R fronal-SFG/SMA, L temporal- ITG, L frontal-IFG, B/L MC*	Discordant	−62	−22	NA

Preictal BOLD changes were seen at $P < 0.05$ (FWE corrected) for two patients, rest of the patients revealed BOLD changes at less conservative statistical threshold $P < 0.001$ uncorrected for FWE only (italicized). The first cluster is the most statistically significant cluster (global-maximum).
B/L = bilateral.

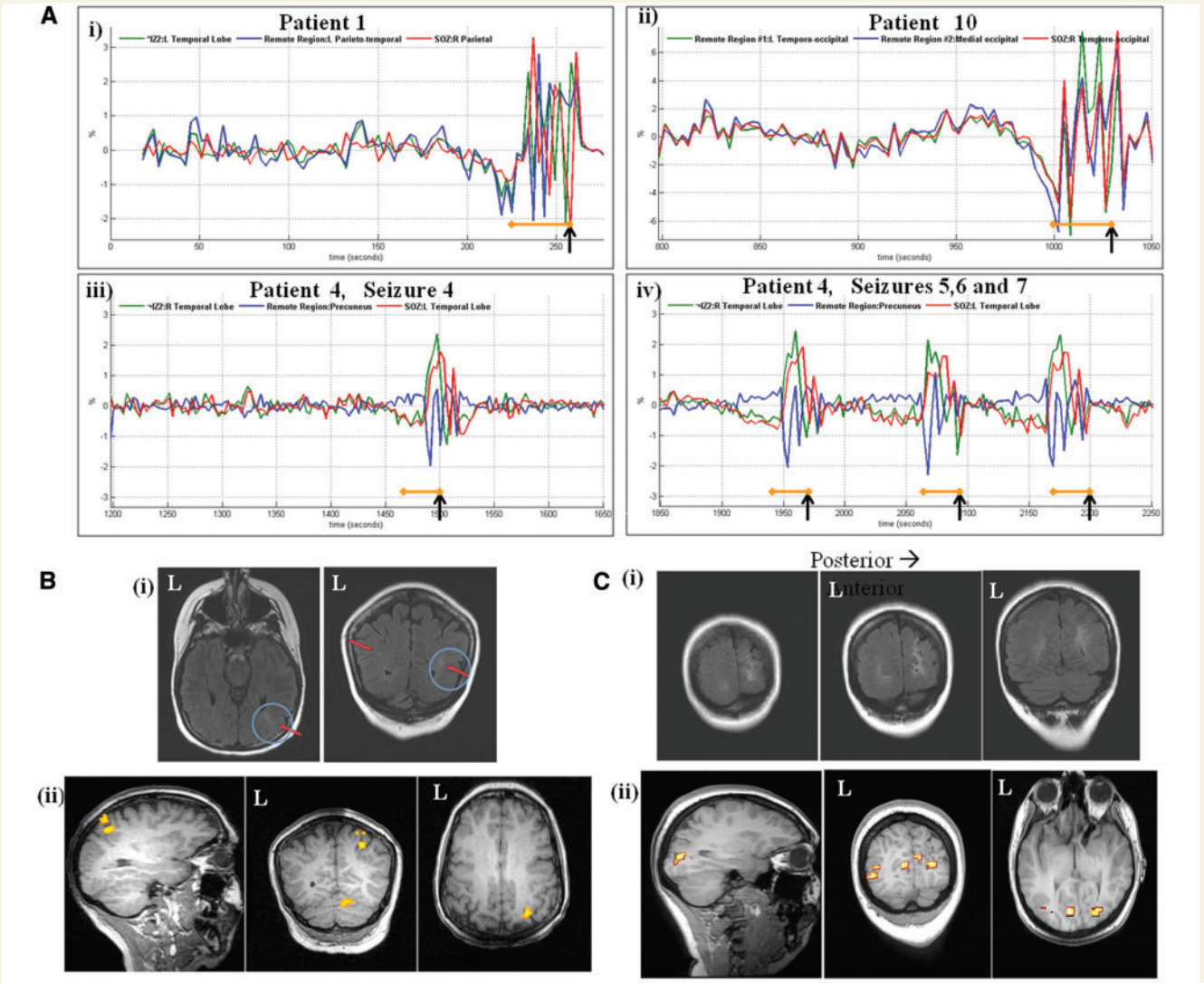

Figure 4 Preictal time courses and BOLD changes. (**A**) Time courses of preictal BOLD clusters for Patients 1, 4 and 10. Before the seizure onset on scalp-EEG, multiple areas including the seizure onset zone, irritative zone and remote regions showed a consistent BOLD decrease (median onset: −31 s; 95% CI −35.7 to −26.3) followed by an increase (median onset: −16 s; 95% CI −18.1 to −13.9), suggesting recruitment of a widespread preictal network. Black arrow = seizure onset; orange bar = 30-s preictal window. Patient 1 had a second irritative zone (IZ2) showing interictal epileptiform discharges on MEG. Patient 4 had a second irritative zone (IZ2) showing interictal epileptiform discharges on MEG. (**B**) Patient 1. (**Bi**) Multiple tubers were seen in right parietal lobe (epileptogenic: encircled) and left temporal lobe. (**Bii**) The preictal map (overlaid on co-registered T_1-volume) was classified as concordant plus showing global-maximum cluster in right parietal lobe within the presumed seizure onset zone. (**C**) Patient 10. (**Ci**) Long-standing ischaemic damage with malformation of gyri in right occipito-parietal region extending into right posterior temporal lobe on MRI scan. (**Cii**) The preictal map (overlaid on co-registered T_1-volume) had some concordance showing global-maximum BOLD cluster in left medial parieto-occipital region and another cluster in right lateral parieto-occipital region within the presumed seizure onset zone.

haemodynamic changes specific to preictal and ictal phases. The main findings of the study are as follows: (i) non-invasive sub-lobar localization of ictal onset phase-related global-maximum cluster within the presumed seizure onset zone, which was confirmed by its comparison with the invasively defined seizure onset zone where available and is superior to the localization provided by scalp-EEG; (ii) propagated BOLD changes in symptomatogenic and resting state network-related areas during seizures; (iii) identification of a consistent pattern of preictal BOLD decrease from −31 s (95% CI −35.7 to −26.3) followed by an increase from −16 s (95% CI −18.1 to −13.9), with a degree of concordance with the seizure onset zone; (iv) predominant onset-related BOLD increases in the seizure onset zone followed by remote BOLD decreases; and (v) utility of simultaneous video recordings for functional MRI studies of seizures.

Previous EEG–functional MRI studies with low yield (Salek-Haddadi *et al*., 2002; Archer *et al*., 2006; Auer *et al*., 2008; Donaire *et al*., 2009; Tyvaert *et al*., 2009; LeVan *et al*., 2010; Thornton *et al*., 2010) have largely recorded seizures fortuitously in the course of studies aimed at mapping interictal epileptiform discharges. In contrast, we have focused on patients with frequent daily seizures, and seizures were identified on the

basis of ictal semiology on video in 15% of patients, as EEG was not helpful, which might have been disregarded in the absence of video.

The concordance of the BOLD maps with the seizure onset zone, in the largest number of seizures investigated with video-EEG–functional MRI, was higher for the ictal onset phase than preictal and later ictal phases, emphasizing the importance of seizure onset localization (ILAE, 1989). The distance between the BOLD clusters and invasively defined seizure onset zone has previously only been measured in one study from our group (Thornton *et al*., 2010), and the proportion of cases with ictal-related BOLD changes concordant with the invasively defined seizure onset zone is higher in this study as compared with Thornton *et al*. (2010).

The BOLD changes in symptomatogenic areas, remote from the seizure onset zone, and in the default mode network-related areas were predominantly decreases. In comparison, the maps concordant with the presumed seizure onset zone for ictal onset/ictal phase predominantly showed increases in line with previous studies of ictal and interictal activity (Tyvaert *et al*., 2008; Donaire *et al*., 2009; Jacobs *et al*., 2009; Vulliemoz *et al*., 2009). In our study, the preictal maps have shown a relatively widespread pattern of changes in line with previous studies in a limited number of cases (Donaire *et al*., 2009; Tyvaert *et al*., 2009).

Methodological considerations

We used intra-scanner synchronized video-EEG to identify seizures (Foldvary *et al*., 2001; Luders *et al*., 2006), which is superior to intra-scanner EEG alone (Tyvaert *et al*., 2008; Thornton *et al*., 2010), owing to difficulties with interpretation (Benar *et al*., 2003). Previously, seizures have been represented, for functional MRI modelling, as single blocks (Tyvaert *et al*., 2008; Salek-Haddadi *et al*., 2009; Bai *et al*., 2010) or contiguous sliding windows (Donaire *et al*., 2009), which are not specifically related to ictal electrophysiology or semiology. We attempted to further improve on our previous modelling approach of EEG-informed seizure blocks (Thornton *et al*., 2010) by dividing seizures into more defined phases on the basis of their spatiotemporal evolution (Niedermeyer and Lopes da Silva, 2005) on video-EEG separating the ictal onset-related changes from the propagated and semiology-associated changes. We used a canonical haemodynamic kernel and its derivatives (Friston *et al*., 1995*b*, 1996) to account for a degree of variability in BOLD timing and shape. We also accounted for motion, cardiac pulse and normal physiological activities in the design matrix more thoroughly than in all previous studies to explain a greater amount of nuisance variance in the functional MRI data to increase sensitivity to the effects of interest (Chaudhary *et al*., 2012). We believe that our results validate this approach.

We represented seizures as a single effect when a patient had more than one seizure of the same type (Wendling *et al*., 1996), reflecting the assumption that they are associated with a consistent BOLD pattern and thereby can potentially increase the statistical power of the functional MRI analysis (Hamandi *et al*., 2006). The successful identification of significant BOLD changes averaged across events in the cases with repeated seizures provides some indication of the core aspects of the ictal networks, and the current approach can further characterize the BOLD changes for the ictal onset and semiology in seizure-related areas.

For the preictal phase, we used a more flexible approach based on the Fourier basis set, which is capable of capturing arbitrarily shaped fluctuations. We think that this approach can be justified by the fact that the exact onset and time course of preictal haemodynamic changes before any behavioural or EEG features are particularly less well defined. We selected a 30-s window to include the timeline of preictal changes as reported in some functional MRI (Donaire *et al*., 2009) and optical imaging studies (Zhao *et al*., 2007). This choice is also partly justified by the desire to use the same duration in all cases and the $\geqslant$1-min inter-seizure interval in our data (except Patients 4, 7 and 11 in whom the inter-seizure interval was $<$30 s, and the preictal phase for the following seizure was not included in the design matrix as a separate event), and to avoid the effects of overlap between the preictal time window and preceding seizures. Additionally, we did not force the Fourier basis set to zero at the start of the preictal window to assess whether the changes are likely to have started $\geqslant$30 s before the seizure onset.

The basis set approach has been used previously to map interictal (Lemieux *et al*., 2008; Masterton *et al*., 2010) and ictal (Thornton *et al*., 2010) BOLD changes. We used Fourier basis set to map preictal BOLD changes because (i) it can capture small deviations from the canonical haemodynamic response better than finite impulse response (Penny *et al*., 2007); (ii) it modelled signal fluctuations taking place for a time scale of $\geqslant$2 repetition times, and limited the effects of noise by constraining the estimated time course with proper assessment of statistical significance within the SPM framework, in contrast to averaging time courses; and (iii) it can reveal preictal changes throughout the brain independently of the results for the later ictal phases, in contrast with methods based on the analysis of the BOLD signal in regions identified ictally (Bai *et al*., 2010). Preictal changes were not explored in patients with reflex focal seizures because seizures were triggered immediately after the stimulus presentation.

We found that the distance between the global-maximum or other BOLD cluster within the presumed seizure onset zone and the invasively defined seizure onset zone ranged from 1.1 to 3.5 cm, which we consider concordant with the seizure onset zone, taking into account possible co-registration inaccuracies due to implantation-related brain shift (Nimsky *et al*., 2000) and neurovascular coupling effects (Disbrow *et al*., 2000). Limitations of this comparison include (i) video-EEG–functional MRI and invasive EEG recordings were performed at different times; (ii) the conditions under which seizures were recorded on invasive EEG were different, e.g. effects of drug reduction, sleep deprivation and anaesthesia; and (iii) invasive EEG has limited spatial sampling. The fundamentally different nature of the two modalities means that the lack of significant BOLD signal change in a given region sampled by invasive EEG does not preclude the occurrence of epileptic activity (Nunez *et al*., 2000; Tyvaert *et al*., 2009).

One of the weaknesses of functional MRI is that it is a correlative technique that often produces complex BOLD maps containing multiple clusters. To address the problem of interpreting the findings, we used a concordance classification (Thornton *et al*.,

2010; Grouiller *et al*., 2011; Chaudhary *et al*., 2012) and conservative statistical threshold. The degree of concordance of the maps was evaluated by comparing the location of the global-maximum and other clusters with the seizure onset zone defined independently. Entirely concordant maps can be taken as 'true positive' findings; concordant plus and some concordance maps as a mixture of 'true and false positive' results and discordant maps as 'false positive'. This approach also embodies the proposition that the global-maximum cluster, which is usually unique for a given map (Friston *et al*., 1995*b*; Friston, 1996; Worsley *et al*., 2002), might have a special biological or clinical significance, as shown by our findings and those of previous studies. Future advances in functional MRI acquisition and modelling may reveal that that the global-maximum cluster is a key marker of epileptogenic networks.

Our approach was motivated by the desire to extract as much information from each and every data set as possible. We found no specific correlation between the ictal BOLD changes and the amount of head motion (Supplementary Appendix III and Supplementary Fig. 1). Moreover, the amount of head motion was comparable with that observed in our previous study of seizures (Thornton *et al*., 2010) but greater than for studies in the interictal state (Salek-Haddadi *et al*., 2006). It can be argued that including all data irrespective of motion may corrupt the functional MRI signal excessively. We suggest that including as thorough a model of confounds as possible and using a concordance scheme can help in the interpretation and limit the false positive findings.

Neurobiological significance

We found sustained BOLD increases predominantly at the seizure onset for the ictal onset/ictal phase and decreases for the later ictal phases, representing seizure spread consistent with previous findings (Donaire *et al*., 2009; Tyvaert *et al*., 2009; Thornton *et al*., 2010). We suggest that BOLD increases can be linked directly to increased neuronal activity (Logothetis *et al*., 2001), and sustained BOLD decreases may represent inhibitory inputs (Shmuel *et al*., 2006), demand and perfusion mismatch (Raichle *et al*., 2001; Zhao *et al*., 2009) or dysregulated neurovascular coupling (Schridde *et al*., 2008). However, many details of the relationship between BOLD and neuronal activity remain to be elucidated further (Pasley *et al*., 2007; Shulman *et al*., 2007).

Interestingly, it has been reported that cerebral blood flow can be compromised in areas of structural abnormalities resulting in BOLD decreases associated with increases in neuronal activity (Sakatani *et al*., 2007). In contrast, we found a mixture of increases and decreases irrespective of the presence of structural abnormality in line with previous studies (Hamandi *et al*., 2006; Laufs *et al*., 2007; Jacobs *et al*., 2009; Vaudano *et al*., 2009; Vulliemoz *et al*., 2009; Thornton *et al*., 2010; Moeller *et al*., 2011).

Preictal maps had a lesser degree of concordance with the seizure onset zone than ictal onset phase-related maps. We found that preictal changes started with a consistent sustained decrease from −31 s (95% CI −35.7 to −26.3) followed by an increase from −16 s (95% CI −18.1 to −13.9) in agreement with Donaire *et al*. (2009); however, Tyvaert *et al*. (2009) found preictal increases preceding decreases at lower statistical threshold. Preictal changes were seen in the seizure onset zone, irritative zones and other remote areas in this work, whereas Donaire *et al*. (2009) found changes in the putative seizure onset zone and the default mode network-related areas. We suggest that the initial BOLD decreases may correspond to the active inhibitory circuits (Wendling *et al*., 2005; Gnatkovsky *et al*., 2008; Trombin *et al*., 2011), which are subsequently overtaken by the increase in neuronal activity driven by glutamatergic neurons (Huberfeld *et al*., 2011). More specifically, preictal changes in remote areas may represent fluctuations in the resting state networks (Schwartz *et al*., 2011) or involvement of wider networks (Bartolomei *et al*., 2001; Truccolo *et al*., 2011) before the seizure onset.

Additionally, ictal patterns on scalp-EEG may be delayed by up to 8 s as compared with invasive EEG, representing propagation (Ray *et al*., 2007). In this study, the first EEG change on invasive EEG preceded the first clinical change by 3–38 s (Table 4) in the six patients who had invasive recordings. This suggests that the preictal changes may hint towards the increase in neuronal activity, which is yet not powerful or synchronized enough to be seen on scalp-EEG (Gavaret *et al*., 2004; Ray *et al*., 2007), since an area of at least 6–10cm^2 is required to be recruited to produce electrical activity on scalp-EEG (Tao *et al*., 2005; Ray *et al*., 2007). It also highlights that metabolic changes may precede overt electrical changes (Donaire *et al*., 2009; Tyvaert *et al*., 2009; Zhao *et al*., 2009). Preictal changes may also reflect preictal discharges (Huberfeld *et al*., 2011), fast oscillatory activity (Wendling *et al*., 2005; Gnatkovsky *et al*., 2008) or activity from glial cells (Moore and Cao, 2008; Figley *et al*., 2011). Further experiments with simultaneous scalp and invasive EEG–functional MRI (Vulliemoz *et al*., 2011) greatly improve our ability to characterize the interictal–ictal transition.

Ictal-related BOLD changes in the resting state networks may reflect neuronal baseline activity (Damoiseaux *et al*., 2006) from which task-related networks are modulated (Mantini *et al*., 2007), or transitions in brain dynamics as a result of ictal discharges, i.e. recruitment during seizure propagation (downstream) or upstream from ictal activity, reflecting changes in brain state favouring seizure occurrences (Vaudano *et al*., 2009).

Clinical significance

We observed ictal onset phase-related BOLD changes concordant with the seizure onset zone in 85% of the cases compared with 44% in Thornton *et al*. (2010). We suggest that this is related to the ability of video-EEG to identify and classify seizures better than EEG alone, leading to improved functional MRI modelling of seizures, the inclusion of regressors for physiological activities and a refined concordance scheme (Chaudhary *et al*., 2012).

We have shown that in 65% of patients, the ictal onset phase-related global-maximum cluster (entirely concordant/concordant plus maps) was co-localized within the presumed seizure onset zone at the sub-lobar, which is superior to scalp-EEG. In the implanted cases in this study, the ictal onset phase-related global-maximum BOLD cluster was 1.1–3.5 cm from the invasively defined seizure onset zone at sub-lobar level. This suggests that video-EEG–functional MRI can capture relevant ictal onset phase-

related localization information. For example, our results show that video-EEG–functional MRI may anticipate situations where invasive EEG is unlikely to be fruitful because of potential surgical sequelae on eloquent cortex, as for Patients 3 and 10 (Fig. 1), and surgical outcome, i.e. ILAE Class I outcome (Patients 1 and 16; Fig. 1) when the ictal onset phase-related BOLD cluster within the presumed seizure onset zone was resected and Class III (Patient 4) when it was not resected. Intracranial EEG is an expensive test and is limited by its unsuitability and the risk of surgical complications in some cases (Knowlton *et al*., 2008*a*, *b*). Non-invasive investigations can help to formulate consensus hypotheses about the seizure generation and spread for the implantation of intracranial electrodes. However, they mostly map the irritative zone (EEG and MEG source imaging and FDG-PET) or may localize the seizure onset zone falsely (ictal SPECT) (Knowlton, 2006, 2009). We suggest that the confirmation of the sub-lobar localization of the ictal onset phase-related global-maximum or other BOLD cluster within the presumed seizure onset zone may be a useful marker in the planning of invasive investigations. However, establishing clinical usefulness will require larger prospective studies to identify predictive power in terms of invasive EEG localization and surgical outcome. It is possible that ictal video-EEG–functional MRI has a negative predictive power similar to interictal EEG–functional MRI (Thornton *et al*., 2011).

In patients who did not have invasive EEG recordings, the presumed seizure onset zone was localized on the basis of structural abnormality on MRI and scalp-EEG or scalp-EEG alone. Additionally, ictal patterns on scalp-EEG from deep brain structures such as the medial temporal (Pacia and Ebersole, 1997) and frontal structures (Jobst *et al*., 2000; Lee *et al*., 2000) are difficult to localize. We suggest that the sub-lobar localization of ictal onset phase-related global-maximum BOLD cluster within the presumed seizure onset zone was superior to the lobar localization of scalp-EEG alone in lesional and non-lesional cases, further refining the localization process.

Ictal established/ictal phase-related BOLD changes in symptomatogenic areas (Swartz 1994; Luders *et al*., 1998; Lee *et al*., 2002; Loddenkemper and Kotagal, 2005; Kameyama *et al*., 2010; Foldvary-Schaefer and Unnwongse, 2011) were revealed in line with our previous work (Thornton *et al*., 2010). The location of these changes broadly reflected ictal semiology, suggesting that they correspond to downstream propagation network (Tyvaert *et al*., 2008; Thornton *et al*., 2010). BOLD changes were also seen in non-symptomatogenic areas in these patients. Future work will focus on ascertaining whether these merely reflect motion-related signal changes or propagation networks involving fluctuations in resting state networks.

It has been suggested that BOLD decreases in the default mode network may be associated with loss of awareness (Laufs *et al*., 2003, 2006; Gotman *et al*., 2005; Bai *et al*., 2010; Berman *et al*., 2010; Carney *et al*., 2010; Moeller *et al*., 2010). We found an association between BOLD decreases in the default mode network in this study and loss of consciousness as assessed during long-term video-EEG monitoring for typical seizures. This may reflect an over-synchronization of electrical activity in associative cortices during the later part of seizures and loss of awareness (Arthuis *et al*., 2009).

The sensitivity of video-EEG–functional MRI to capture seizures in this study was 36% compared with 4% in Tyvaert *et al*. (2008) and 11% in Thornton *et al*. (2010), which may be because of a strict selection criteria. The need to scan in real time combined with limited access to scan time is likely to limit the technique's clinical utility based on current scanner technology and places it on a par with MEG. The technique is at a disadvantage compared with ictal SPECT in this regard. However video-EEG–functional MRI is more suited to the study of interictal–ictal transition and ictal onset specifically.

We cannot address specificity rigorously considering the small number of patients studied. In our centre and many others, invasive EEG is considered the gold standard to localize the seizure onset zone (Rosenow and Luders, 2001; Luders *et al*., 2006). The question of the nature and biological significance of the areas active at the seizure onset: single region (Luders *et al*., 2006), or the network concept (Bartolomei *et al*., 2001; Spencer, 2002; Truccolo *et al*., 2011), may have implications for the interpretation of our results. Answering this question would require complete characterization of the seizure onset zone beyond currently available means. Given the current presurgical evaluation techniques, we believe that the approach used here remains the most appropriate way of summarizing the relationship between the BOLD maps and independently obtained localizing information.

In conclusion, simultaneous video-EEG–functional MRI can reveal haemodynamic changes specifically related to the preictal phase, seizure onset and evolution and resting state BOLD networks recruited during seizures, in a significant proportion of patients with frequent seizures. Ictal onset phase-related BOLD changes are often co-localized with the invasively defined seizure onset zone, therefore providing useful non-invasive information to guide invasive investigations in some cases and avoid unnecessary implantations in others.

Acknowledgements

The authors thank Elaine Williams and Jane Burdett for their help with MRI scanning and Teresa Murta for her help with preparing Fig. 4.

Funding

Medical Research Council (MRC grant number G0301067), Action Medical Research, Higher Education Commission of Pakistan, SNF grant 33CM30-124089 (SPUM Epilepsy) from the Swiss National Science Foundation and UCL Institute of Neurology. This work was undertaken at UCLH/UCL, which received a proportion of funding from the Department of Health's NIHR Biomedical Research Centres funding scheme. The authors are grateful to the Big Lottery Fund, Wolfson Trust and the Epilepsy Society for supporting the MRI scanner.

Supplementary material

Supplementary material is available at *Brain* online.

References

Allen PJ, Josephs O, Turner R. A method for removing imaging artifact from continuous EEG recorded during functional MRI. Neuroimage 2000; 12: 230–9.

Allen PJ, Polizzi G, Krakow K, Fish DR, Lemieux L. Identification of EEG events in the MR scanner: the problem of pulse artifact and a method for its subtraction. Neuroimage 1998; 8: 229–39.

Archer JS, Waites AB, Abbott DF, Federico P, Jackson GD. Event-related fMRI of myoclonic jerks arising from dysplastic cortex. Epilepsia 2006; 47: 1487–92.

Arthuis M, Valton L, Regis J, Chauvel P, Wendling F, Naccache L, et al. Impaired consciousness during temporal lobe seizures is related to increased long-distance cortical-subcortical synchronization. Brain 2009; 132: 2091–101.

Auer T, Veto K, Doczi T, Komoly S, Juhos V, Janszky J, et al. Identifying seizure-onset zone and visualizing seizure spread by fMRI: a case report. Epileptic Disord 2008; 10: 93–100.

Bai X, Vestal M, Berman R, Negishi M, Spann M, Vega C, et al. Dynamic time course of typical childhood absence seizures: EEG, behavior, and functional magnetic resonance imaging. J Neurosci 2010; 30: 5884–93.

Barba C, Barbati G, Minotti L, Hoffmann D, Kahane P. Ictal clinical and scalp-EEG findings differentiating temporal lobe epilepsies from temporal 'plus' epilepsies. Brain 2007; 130: 1957–67.

Bartolomei F, Wendling F, Bellanger JJ, Regis J, Chauvel P. Neural networks involving the medial temporal structures in temporal lobe epilepsy. Clin Neurophysiol 2001; 112: 1746–60.

Benar C, Aghakhani Y, Wang Y, Izenberg A, Al-Asmi A, Dubeau F, et al. Quality of EEG in simultaneous EEG-fMRI for epilepsy. Clin Neurophysiol 2003; 114: 569–80.

Berman R, Negishi M, Vestal M, Spann M, Chung MH, Bai X, et al. Simultaneous EEG, fMRI, and behavior in typical childhood absence seizures. Epilepsia 2010; 51: 2011–22.

Binnie CD, Stefan H. Modern electroencephalography: its role in epilepsy management. Clin Neurophysiol 1999; 110: 1671–97.

Carney PW, Masterton RA, Harvey AS, Scheffer IE, Berkovic SF, Jackson GD. The core network in absence epilepsy. Differences in cortical and thalamic BOLD response. Neurology 2010; 75: 904–11.

Catarino CB, Vollmar C, Noachtar S. Paradoxical lateralization of non-invasive electroencephalographic ictal patterns in extra-temporal epilepsies. Epilepsy Res 2012; 99: 147–55.

Centeno M, Feldmann M, Harrison NA, Rugg-Gunn FJ, Chaudhary U, Falcon C, et al. Epilepsy causing pupillary hippus: an unusual semiology. Epilepsia 2011; 52: e93–6.

Chaudhary UJ, Duncan JS, Lemieux L. Mapping hemodynamic correlates of seizures using fMRI: a review. Hum Brain Mapp 2011. Advance Access published on November 14, 2011, doi: 10.1002/hbm.21448.

Chaudhary UJ, Kokkinos V, Carmichael DW, Rodionov R, Gasston D, Duncan JS, et al. Implementation and evaluation of simultaneous video-electroencephalography and functional magnetic resonance imaging. Magn Reson Imaging 2010; 28: 1192–9.

Chaudhary UJ, Rodionov R, Carmichael DW, Thornton RC, Duncan JS, Lemieux L. Improving the sensitivity of EEG-fMRI studies of epileptic activity by modelling eye blinks, swallowing and other video-EEG detected physiological confounds. Neuroimage 2012; 61: 1383–93.

Damoiseaux JS, Rombouts SA, Barkhof F, Scheltens P, Stam CJ, Smith SM, et al. Consistent resting-state networks across healthy subjects. Proc Natl Acad Sci USA 2006; 103: 13848–53.

Detre JA, Sirven JI, Alsop DC, O'Connor MJ, French JA. Localization of subclinical ictal activity by functional magnetic resonance imaging: correlation with invasive monitoring. Ann Neurol 1995; 38: 618–24.

Disbrow EA, Slutsky DA, Roberts TP, Krubitzer LA. Functional MRI at 1.5 tesla: a comparison of the blood oxygenation level-dependent signal and electrophysiology. Proc Natl Acad Sci USA 2000; 97: 9718–23.

Donaire A, Bargallo N, Falcon C, Maestro I, Carreno M, Setoain J, et al. Identifying the structures involved in seizure generation using sequential analysis of ictal-fMRI data. Neuroimage 2009; 47: 173–83.

Duncan JS. Imaging in the surgical treatment of epilepsy. Nat Rev Neurol 2010; 6: 537–50.

Federico P, Abbott DF, Briellmann RS, Harvey AS, Jackson GD. Functional MRI of the preictal state. Brain 2005; 128: 1811–7.

Figley CR, Stroman PW. The role(s) of astrocytes and astrocyte activity in neurometabolism, neurovascular coupling, and the production of functional neuroimaging signals. Eur J Neurosci 2011; 33: 577–88.

Foldvary N, Klem G, Hammel J, Bingaman W, Najm I, Luders H. The localizing value of ictal EEG in focal epilepsy. Neurology 2001; 57: 2022–8.

Foldvary-Schaefer N, Unnwongse K. Localizing and lateralizing features of auras and seizures. Epilepsy Behav 2011; 20: 160–6.

Friston KJ. Statistical parametric mapping and other analyses of functional imaging data. In: Toga AW, Mazziotta JC, editors. Brain mapping: the methods. San Diego: Academic Press; 1996. p. 363–96.

Friston KJ, Ashburner J, Frith C, Poline JB, Heather JD, Frackowiak RSJ. Spatial registration and normalization of images. Hum Brain Mapp 1995a; 3: 165–89.

Friston KJ, Holmes AP, Worsley KJ, Poline JB, Firth CD, Frackowiak RSJ. Statistical parametric maps in functional imaging: a general linear approach. Hum Brain Mapp 1995b; 2: 189–210.

Friston KJ, Williams S, Howard R, Frackowiak RS, Turner R. Movement-related effects in fMRI time-series. Magn Reson Med 1996; 35: 346–55.

Gavaret M, McGonigal A, Badier JM, Chauvel P. Physiology of frontal lobe seizures: preictal, ictal and interictal relationships. Suppl Clin Neurophysiol 2004; 57: 400–7.

Gnatkovsky V, Librizzi L, Trombin F, de CM. Fast activity at seizure onset is mediated by inhibitory circuits in the entorhinal cortex in vitro. Ann Neurol 2008; 64: 674–86.

Gotman J, Grova C, Bagshaw A, Kobayashi E, Aghakhani Y, Dubeau F. Generalized epileptic discharges show thalamocortical activation and suspension of the default state of the brain. Proc Natl Acad Sci USA 2005; 102: 15236–40.

Grouiller F, Thornton RC, Groening K, Spinelli L, Duncan JS, Schaller K, et al. With or without spikes: localization of focal epileptic activity by simultaneous electroencephalography and functional magnetic resonance imaging. Brain 2011; 134: 2867–86.

Hamandi K, Salek-Haddadi A, Laufs H, Liston A, Friston K, Fish DR, et al. EEG-fMRI of idiopathic and secondarily generalized epilepsies. Neuroimage 2006; 31: 1700–10.

Huberfeld G, dlP Menendez, Pallud J, Cohen I, Le Van QM, Adam C, et al. Glutamatergic preictal discharges emerge at the transition to seizure in human epilepsy. Nat Neurosci 2011; 14: 627–34.

ILAE. Proposal for revised classification of epilepsies and epileptic syndromes. Commission on classification and terminology of the International League Against Epilepsy. Epilepsia 1989; 30: 389–99.

Jackson GD, Connelly A, Cross JH, Gordon I, Gadian DG. Functional magnetic resonance imaging of focal seizures. Neurology 1994; 44: 850–6.

Jacobs J, LeVan P, Moeller F, Boor R, Stephani U, Gotman J, et al. Hemodynamic changes preceding the interictal EEG spike in patients with focal epilepsy investigated using simultaneous EEG-fMRI. Neuroimage 2009; 45: 1220–31.

Jobst BC, Siegel AM, Thadani VM, Roberts DW, Rhodes HC, Williamson PD. Intractable seizures of frontal lobe origin: clinical characteristics, localizing signs, and results of surgery. Epilepsia 2000; 41: 1139–52.

Kameyama S, Masuda H, Murakami H. Ictogenesis and symptomatogenesis of gelastic seizures in hypothalamic hamartomas: an ictal SPECT study. Epilepsia 2010; 51: 2270–9.

Katschnig P, Schwingenschuh P, Chaudhary UJ, Edwards MJ, Lemieux L, Walker MC, et al. Paroxysmal limb dyskinesia induced by weight: an unusual case of cortical reflex seizures. Mov Disord 2011; 26: 2438–9.

Knowlton RC. The role of FDG-PET, ictal SPECT, and MEG in the epilepsy surgery evaluation. Epilepsy Behav 2006; 8: 91–101.

Knowlton RC, Elgavish RA, Bartolucci A, Ojha B, Limdi N, Blount J, et al. Functional imaging: II. Prediction of epilepsy surgery outcome. Ann Neurol 2008a; 64: 35–41.

Knowlton RC, Elgavish RA, Limdi N, Bartolucci A, Ojha B, Blount J, et al. Functional imaging: I. Relative predictive value of intracranial electroencephalography. Ann Neurol 2008b; 64: 25–34.

Knowlton RC, Razdan SN, Limdi N, Elgavish RA, Killen J, Blount J, et al. Effect of epilepsy magnetic source imaging on intracranial electrode placement. Ann Neurol 2009; 65: 716–23.

Krings T, Topper R, Reinges MH, Foltys H, Spetzger U, Chiappa KH, et al. Hemodynamic changes in simple partial epilepsy: a functional MRI study. Neurology 2000; 54: 524–7.

Kubota F, Kikuchi S, Ito M, Shibata N, Akata T, Takahashi A, et al. Ictal brain hemodynamics in the epileptic focus caused by a brain tumor using functional magnetic resonance imaging (fMRI). Seizure 2000; 9: 585–9.

Laufs H, Hamandi K, Salek-Haddadi A, Kleinschmidt AK, Duncan JS, Lemieux L. Temporal lobe interictal epileptic discharges affect cerebral activity in "default mode" brain regions. Hum Brain Mapp 2007; 28: 1023–32.

Laufs H, Krakow K, Sterzer P, Eger E, Beyerle A, Salek-Haddadi A, et al. Electroencephalographic signatures of attentional and cognitive default modes in spontaneous brain activity fluctuations at rest. Proc Natl Acad Sci USA 2003; 100: 11053–8.

Laufs H, Lengler U, Hamandi K, Kleinschmidt A, Krakow K. Linking generalized spike-and-wave discharges and resting state brain activity by using EEG/fMRI in a patient with absence seizures. Epilepsia 2006; 47: 444–8.

Lee KH, Meador KJ, Park YD, King DW, Murro AM, Pillai JJ, et al. Pathophysiology of altered consciousness during seizures: subtraction SPECT study. Neurology 2002; 59: 841–6.

Lee SK, Kim JY, Hong KS, Nam HW, Park SH, Chung CK. The clinical usefulness of ictal surface EEG in neocortical epilepsy. Epilepsia 2000; 41: 1450–5.

Lemieux L, Laufs H, Carmichael D, Paul JS, Walker MC, Duncan JS. Noncanonical spike-related BOLD responses in focal epilepsy. Hum Brain Mapp 2008; 29: 329–45.

Lemieux L, Salek-Haddadi A, Lund TE, Laufs H, Carmichael D. Modelling large motion events in fMRI studies of patients with epilepsy. Magn Reson Imaging 2007; 25: 894–901.

LeVan P, Tyvaert L, Moeller F, Gotman J. Independent component analysis reveals dynamic ictal BOLD responses in EEG-fMRI data from focal epilepsy patients. Neuroimage 2010; 49: 366–78.

Liston AD, Lund TE, Salek-Haddadi A, Hamandi K, Friston KJ, Lemieux L. Modelling cardiac signal as a confound in EEG-fMRI and its application in focal epilepsy studies. Neuroimage 2006; 30: 827–34.

Loddenkemper T, Kotagal P. Lateralizing signs during seizures in focal epilepsy. Epilepsy Behav 2005; 7: 1–17.

Logothetis NK, Pauls J, Augath M, Trinath T, Oeltermann A. Neurophysiological investigation of the basis of the fMRI signal. Nature 2001; 412: 150–7.

Luders H, Acharya J, Baumgartner C, Benbadis S, Bleasel A, Burgess R, et al. Semiological seizure classification. Epilepsia 1998; 39: 1006–13.

Luders H, Comair YG. Epilepsy surgery. Philadelphia: Lippincott Williams & Wilkins; 2000a.

Luders H, Noachtar S, Benson JK. Atlas and classification of electroencephalography. Philadelphia: Saunders; 2000b.

Luders HO, Najm I, Nair D, Widdess-Walsh P, Bingman W. The epileptogenic zone: general principles. Epileptic Disord 2006; 8 (Suppl 2): S1–9.

Mantini D, Perrucci MG, Del GC, Romani GL, Corbetta M. Electrophysiological signatures of resting state networks in the human brain. Proc Natl Acad Sci USA 2007; 104: 13170–5.

Masterton RA, Harvey AS, Archer JS, Lillywhite LM, Abbott DF, Scheffer IE, et al. Focal epileptiform spikes do not show a canonical BOLD response in patients with benign rolandic epilepsy (BECTS). Neuroimage 2010; 51: 252–60.

Moeller F, LeVan P, Gotman J. Independent component analysis (ICA) of generalized spike wave discharges in fMRI: comparison with general linear model-based EEG-fMRI. Hum Brain Mapp 2011; 32: 209–17.

Moeller F, Muhle H, Wiegand G, Wolff S, Stephani U, Siniatchkin M. EEG-fMRI study of generalized spike and wave discharges without transitory cognitive impairment. Epilepsy Behav 2010; 18: 313–6.

Moore CI, Cao R. The hemo-neural hypothesis: on the role of blood flow in information processing. J Neurophysiol 2008; 99: 2035–47.

Niedermeyer E, Lopes da Silva FH. Electroencephalography: basic principles, clinical applications, and related fields. Philadelphia: Lippincott Williams & Wilkins; 2005.

Nimsky C, Ganslandt O, Cerny S, Hastreiter P, Greiner G, Fahlbusch R. Quantification of, visualization of, and compensation for brain shift using intraoperative magnetic resonance imaging. Neurosurgery 2000; 47: 1070–9.

Nunez PL, Silberstein RB. On the relationship of synaptic activity to macroscopic measurements: does co-registration of EEG with fMRI make sense? Brain Topogr 2000; 13: 79–96.

Pacia SV, Ebersole JS. Intracranial EEG substrates of scalp ictal patterns from temporal lobe foci. Epilepsia 1997; 38: 642–54.

Pasley BN, Inglis BA, Freeman RD. Analysis of oxygen metabolism implies a neural origin for the negative BOLD response in human visual cortex. Neuroimage 2007; 36: 269–76.

Penny W, Flandin G, Trujillo-Barreto N. Bayesian comparison of spatially regularised general linear models. Hum Brain Mapp 2007; 28: 275–93.

Raichle ME, MacLeod AM, Snyder AZ, Powers WJ, Gusnard DA, Shulman GL. A default mode of brain function. Proc Natl Acad Sci USA 2001; 98: 676–82.

Ray A, Tao JX, Hawes-Ebersole SM, Ebersole JS. Localizing value of scalp EEG spikes: a simultaneous scalp and intracranial study. Clin Neurophysiol 2007; 118: 69–79.

Remi J, Vollmar C, de MA, Heinlin J, Peraud A, Noachtar S. Congruence and discrepancy of interictal and ictal EEG with MRI lesions in focal epilepsies. Neurology 2011; 77: 1383–90.

Rosenow F, Luders H. Presurgical evaluation of epilepsy. Brain 2001; 124: 1683–700.

Sakatani K, Murata Y, Fujiwara N, Hoshino T, Nakamura S, Kano T, et al. Comparison of blood-oxygen-level-dependent functional magnetic resonance imaging and near-infrared spectroscopy recording during functional brain activation in patients with stroke and brain tumors. J Biomed Opt 2007; 12: 062110.

Salek-Haddadi A, Diehl B, Hamandi K, Merschhemke M, Liston A, Friston K, et al. Hemodynamic correlates of epileptiform discharges: an EEG-fMRI study of 63 patients with focal epilepsy. Brain Res 2006; 1088: 148–66.

Salek-Haddadi A, Mayer T, Hamandi K, Symms M, Josephs O, Fluegel D, et al. Imaging seizure activity: a combined EEG/EMG-fMRI study in reading epilepsy. Epilepsia 2009; 50: 256–64.

Salek-Haddadi A, Merschhemke M, Lemieux L, Fish DR. Simultaneous EEG-correlated ictal fMRI. Neuroimage 2002; 16: 32–40.

Schridde U, Khubchandani M, Motelow JE, Sanganahalli BG, Hyder F, Blumenfeld H. Negative BOLD with large increases in neuronal activity. Cereb Cortex 2008; 18: 1814–27.

Schwartz TH, Hong SB, Bagshaw AP, Chauvel P, Benar CG. Preictal changes in cerebral haemodynamics: review of findings and insights from intracerebral EEG. Epilepsy Res 2011; 97: 252–66.

Shmuel A, Augath M, Oeltermann A, Logothetis NK. Negative functional MRI response correlates with decreases in neuronal activity in monkey visual area V1. Nat Neurosci 2006; 9: 569–77.

Shulman RG, Rothman DL, Hyder F. A BOLD search for baseline. Neuroimage 2007; 36: 277–81.

Smith SJ. EEG in the diagnosis, classification, and management of patients with epilepsy. J Neurol Neurosurg Psychiatry 2005; 76 (Suppl 2): ii2–7.

Spencer SS. Neural networks in human epilepsy: evidence of and implications for treatment. Epilepsia 2002; 43: 219–27.

Swartz BE. Electrophysiology of bimanual-bipedal automatisms. Epilepsia 1994; 35: 264–74.

Tao JX, Ray A, Hawes-Ebersole S, Ebersole JS. Intracranial EEG substrates of scalp EEG interictal spikes. Epilepsia 2005; 46: 669–76.

Thornton R, Vulliemoz S, Rodionov R, Carmichael DW, Chaudhary UJ, Diehl B, et al. Epileptic networks in focal cortical dysplasia revealed using electroencephalography-functional magnetic resonance imaging. Ann Neurol 2011; 70: 822–37.

Thornton RC, Rodionov R, Laufs H, Vulliemoz S, Vaudano A, Carmichael D, et al. Imaging haemodynamic changes related to seizures: comparison of EEG-based general linear model, independent component analysis of fMRI and intracranial EEG. Neuroimage 2010; 53: 196–205.

Trombin F, Gnatkovsky V, de CM. Changes in action potential features during focal seizure discharges in the entorhinal cortex of the in vitro isolated guinea pig brain. J Neurophysiol 2011; 106: 1411–23.

Truccolo W, Donoghue JA, Hochberg LR, Eskandar EN, Madsen JR, Anderson WS, et al. Single-neuron dynamics in human focal epilepsy. Nat Neurosci 2011; 14: 635–41.

Tyvaert L, Hawco C, Kobayashi E, LeVan P, Dubeau F, Gotman J. Different structures involved during ictal and interictal epileptic activity in malformations of cortical development: an EEG-fMRI study. Brain 2008; 131: 2042–60.

Tyvaert L, LeVan P, Dubeau F, Gotman J. Noninvasive dynamic imaging of seizures in epileptic patients. Hum Brain Mapp 2009; 30: 3993–4011.

van den Heuvel MP, Mandl RC, Kahn RS, Hulshoff Pol HE. Functionally linked resting-state networks reflect the underlying structural connectivity architecture of the human brain. Hum Brain Mapp 2009; 30: 3127–41.

Vaudano AE, Laufs H, Kiebel SJ, Carmichael DW, Hamandi K, Guye M, et al. Causal hierarchy within the thalamo-cortical network in spike and wave discharges. PLoS One 2009; 4: e6475.

Vulliemoz S, Carmichael DW, Rosenkranz K, Diehl B, Rodionov R, Walker MC, et al. Simultaneous intracranial EEG and fMRI of interictal epileptic discharges in humans. Neuroimage 2011; 54: 182–90.

Vulliemoz S, Thornton R, Rodionov R, Carmichael DW, Guye M, Lhatoo S, et al. The spatio-temporal mapping of epileptic networks: combination of EEG-fMRI and EEG source imaging. Neuroimage 2009; 46: 834–43.

Wendling F, Bellanger JJ, Badier JM, Coatrieux JL. Extraction of spatio-temporal signatures from depth EEG seizure signals based on objective matching in warped vectorial observations. IEEE Trans Biomed Eng 1996; 43: 990–1000.

Wendling F, Hernandez A, Bellanger JJ, Chauvel P, Bartolomei F. Interictal to ictal transition in human temporal lobe epilepsy: insights from a computational model of intracerebral EEG. J Clin Neurophysiol 2005; 22: 343–56.

Worsley KJ, Liao CH, Aston J, Petre V, Duncan GH, Morales F, et al. A general statistical analysis for fMRI data. Neuroimage 2002; 15: 1–15.

Zhao M, Ma H, Suh M, Schwartz TH. Spatiotemporal dynamics of perfusion and oximetry during ictal discharges in the rat neocortex. J Neurosci 2009; 29: 2814–23.

Zhao M, Suh M, Ma H, Perry C, Geneslaw A, Schwartz TH. Focal increases in perfusion and decreases in hemoglobin oxygenation precede seizure onset in spontaneous human epilepsy. Epilepsia 2007; 48: 2059–67.

Zijlmans M, Huiskamp G, Hersevoort M, Seppenwoolde JH, van Huffelen AC, Leijten FS. EEG-fMRI in the preoperative work-up for epilepsy surgery. Brain 2007; 130: 2343–53.